REPORT DOCUMENTATION PAGE

Form Approved
OMB No. 0704-0188

1. REPORT DATE *(DD-MM-YYYY)*	**2. REPORT TYPE**	**3. DATES COVERED** *(From - To)*
05-10-2013		

4. TITLE AND SUBTITLE

Numerical Model for Predicting and Managing Heat Dissipation from a Neural Probe

5a. CONTRACT NUMBER

5b. GRANT NUMBER

5c. PROGRAM ELEMENT NUMBER

6. AUTHOR(S)
Christian, Matthew Paul

5d. PROJECT NUMBER

5e. TASK NUMBER

5f. WORK UNIT NUMBER

7. PERFORMING ORGANIZATION NAME(S) AND ADDRESS(ES)

8. PERFORMING ORGANIZATION REPORT NUMBER

9. SPONSORING / MONITORING AGENCY NAME(S) AND ADDRESS(ES)
U.S. Naval Academy
Annapolis, MD 21402

10. SPONSOR/MONITOR'S ACRONYM(S)

11. SPONSOR/MONITOR'S REPORT NUMBER(S)
Trident Scholar Report no. 411 (2013)

12. DISTRIBUTION / AVAILABILITY STATEMENT

This document has been approved for public release; its distribution is UNLIMITED.

13. SUPPLEMENTARY NOTES

14. ABSTRACT

Stimulating neural probes are used in an effort to better understand neural pathways. Current designs with light as a stimulating impulse externally couple the light into the probe. Relocating the light source to the probe tip would improve the flexibility of the technique; however, this approach would generate heat within the embedded probe. Minor temperature excursions can easily damage tissues under study, creating inaccurate results and/or damaging the tissue. A model has been created using COMSOL for the thermal effects of these heated probes in the brain. The model includes blood perfusion and metabolic processes. The model was used to investigate the effect of different geometric parameters on the temperature excursion as well as the effect of injecting saline solution through the probe to determine if active cooling is a feasible concept in the context of microneural probes. It was observed that the maximum temperature change decreases with insertion depth and decreases as the heated area of the probe is increased. The model was also used to study the effect of extending the probe beyond the heated region. This resulted in a significant reduction in temperature excursion. The model has been experimentally validated through physical tests using an Agar gel as a neural tissue simulant.

15. SUBJECT TERMS
neural probes, bioheat transfer, finite element analysis, modelin, injected fluid flow

16. SECURITY CLASSIFICATION OF:			**17. LIMITATION OF ABSTRACT**	**18. NUMBER OF PAGES**	**19a. NAME OF RESPONSIBLE PERSON**
a. REPORT	**b. ABSTRACT**	**c. THIS PAGE**		31	**19b. TELEPHONE NUMBER** *(include area code)*

U.S.N.A. --- Trident Scholar project report; no. 411 (2013)

NUMERICAL MODEL FOR PREDICTING AND MANAGING HEAT DISSIPATION FROM A NEURAL PROBE

by

Midshipman 1/c Matthew P. Christian
United States Naval Academy
Annapolis, Maryland

Certification of Advisers' Approval

Associate Professor Samara L. Firebaugh
Electrical and Computer Engineering Department

Associate Professor Andrew N. Smith
Mechanical Engineering Department

Acceptance for the Trident Scholar Committee

Professor Maria J. Schroeder
Associate Director of Midshipman Research

USNA-1531-2

Abstract — Stimulating neural probes are used in an effort to better understand neural pathways. Current designs with light as a stimulating impulse externally couple the light into the probe. Relocating the light source to the probe tip would improve the flexibility of the technique; however, this approach would generate heat within the embedded probe. Minor temperature excursions can easily damage tissues under study, creating inaccurate results and/or damaging the tissue. A model has been created using COMSOL for the thermal effects of these heated probes in the brain. The model includes blood perfusion and metabolic processes. The model was used to investigate the effect of different geometric parameters on the temperature excursion as well as the effect of injecting saline solution through the probe to determine if active cooling is a feasible concept in the context of microneural probes. It was observed that the maximum temperature change decreases with insertion depth and decreases as the heated area of the probe is increased. The model was also used to study the effect of extending the probe beyond the heated region. This resulted in a significant reduction in temperature excursion. The model has been experimentally validated through physical tests using an Agar gel as a neural tissue simulant.

Keywords—neural probes; bioheat transfer; finite element analysis; modelin; injected fluid flow

ACKNOWLEDGMENT

This work was made possible by the United States Naval Academy Trident Program, an undergraduate independent research program. The Trident Scholar Committee has provided the opportunity and support for those of us who have had the privilege of participating in this program. Technical assistance has also been provided by Dr. Brian Jamieson and Andrea Pais at Scientific and Biomedical Microsystems. In addition, Dr. Jamieson and his staff provided the most critical material of this investigation, the probes, in order to further examine the effects of possible cooling designs and validate the mathematical models via physical experimentation.

Special thanks go to my Advisers, Professor Firebaugh and Professor Smith, for their continued support and patience throughout this project. Their technical expertise and advice have been an invaluable asset. Additionally, the United States Naval Academy Electrical Engineering and Mechanical Engineering Lab Technicians have been extremely accommodating and helpful throughout the year as I have asked for help and assistance in everything from learning how to solder correctly to arranging the experimental apparatus. Lastly, the USNA Computer Support Branch in Rickover hall has been extremely patient with this project and without their expertise, I would not have had a stable software platform to even model the simplest parts of this work. Many people have been involved in the completion of this project, and I greatly appreciate every bit of support that I received throughout the year.

Contents

I. INTRODUCTION

The manner in which the brain functions is still relatively unknown and has therefore been the subject of extensive research in recent years. Neurons function as a result of an electrochemical phenomenon known as the action potential. In essence, an action potential is an electrical signal that travels down the axon of the neuron towards the axon terminal, where the electrical signal is converted to a chemical signal, which then crosses the space known as the synaptic cleft to interact with other neurons. This action potential is initiated via a disturbance in a neuron's resting membrane potential [1]. The resting potential is maintained by an ion concentration gradient between the two sides of the membrane, which causes what could be described as an ion "pressure" that determines the rate ions enter given a certain permeability

(such as an open ion channel) [1]. When a stimulus acts upon a neuron, small ion channel proteins open, allowing a certain amount of ion influx or efflux, depending on the type of stimulus and the affected channel. An excitatory stimulus will open a sodium channel, increasing sodium ion permeability and causing an influx from the extracellular matrix, thereby reducing the cell's electrochemical membrane potential from approximately -70 mV to some value lower in magnitude. An inhibitory stimulus will cause a potassium channel to open, thereby causing an efflux of K^+ and therefore a hyperpolarization of the membrane to an even more negative value. If enough excitatory stimuli act together, the membrane will be depolarized to roughly -55 mV, causing the electrical signal known as an action potential to travel down the axon as described before [1]. This is the basic process used by neurons to integrate and disseminate information to other neurons in the brain through the neural networks. Emotion, muscle movement, and consciousness are all controlled in essence by these electrical action potentials. Neurons are typically 10-30 μm across at the body and 1 μm across at the axon [2].

Neuroscientists use neural probes, generally needles with microscale metallic electrodes patterned on the surface, to study these neural networks. Figure 1 illustrates a typical neural probe. Probes are typically between 60 and 200 μm wide and 15 to 30 μm thick [2]. These probes are generally comprised of multiple electrodes along the shank with contact patches at the base for recording. The electrodes are used to either electrically stimulate the neurons or monitor their electrical activity.

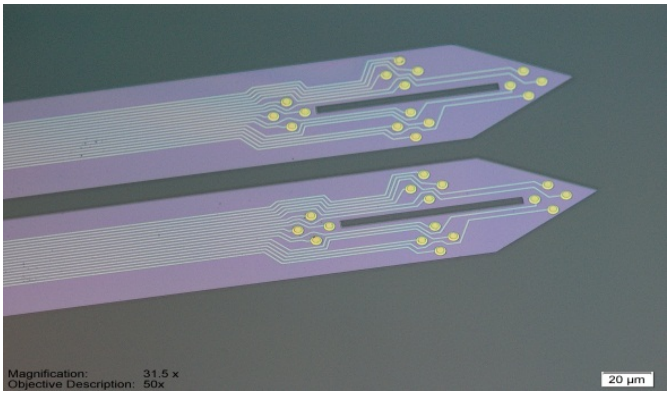

Figure 1: Neural probes containing sensing electrodes. Figure provided by SB Microsystems and reproduced with permission.

While depolarizations can be caused by coupling current through an electrode into neural

tissue, this method lacks spatial specificity by causing other neurons to fire in response to the stimulus. Additionally, the large current transient interferes with recording the response signals causing a lack of temporal resolution. This can confuse the results of the research and make accurate neural mapping difficult [3], [4]. Another issue with electrical neural probes is that they may cause both Joule heating and metabolically-based temperature increases in neural tissue [5]. Temperature increases as low as 0.5 °C can cause changes in cell function [5].

One solution to the problems introduced by electrical stimulation is the use of the channelrhodopsin-2 (ChR2) light-gated ion channel. When illuminated by light of the proper wavelength and intensity, these channels open, increasing permeability to sodium ions, causing a depolarization of the somatic membrane. This protein can be selectively coded and expressed in certain neurons as prescribed by the needs of the research being conducted via genetic engineering methods [3]. With this "optogenetic" technology method, only those neurons desired for study are targeted by the insertion system, therefore subsequent tests will affect only those neurons expressing the ChR2 protein. Neural probes that couple the use of the ChR2 light-stimulated protein and electrode sensing technology allow nearly simultaneous stimulation and recording of neurons attached to the probes since there is no delay between the stimulation signal and the recording signals, as is present in electrically-stimulated systems.

Current technology in optical neural probe design employs the coupling of externally sourced light with a fiber optic system linked to a waveguide through the probe tip, providing the ability to simultaneously stimulate and record activity in neurons expressing the ChR2 channel [4], [6].

Yoon and his colleagues cite the new design's ability to illuminate neurons with specificity, allowing neurons located outside the view of a microscope's objective field of view to be stimulated, thereby allowing more advanced networks to be investigated [4]. The issue with this system is that large networks on multiple brain centers or even multiple animals are difficult to create due to the large fiber jacket coming off of the back of the probe. Also, multiple sources are required if a different firing rate or intensity level is required for each attached probe.

The incorporation of optical sources for stimulating neurons into neural probes enhances their temporal resolution and target specificity [3], [4]. The practical development of these probes is still in its infancy, but research is being done on the most effective way to create light emitting sources small enough to fit on the tip of these probes. Current examples include micro-led systems, such as the micro-array created by Grossman et al [7]. However, the local

generation of the light on the probe could result in more heating than the electrical probes alone, requiring the addition of a thermal management system. In addition, other groups are investigating probes that intentionally introduce a thermal change for either scientific or therapeutic use [8]. A model for the thermal effects of such probes would provide a powerful tool in the design of such systems.

II. Theory and Model Development

A. The Pennes' Bioheat Equation

The Pennes' Bioheat equation, outlined by Wissler [9] and featured in the COMSOL heat transfer module [10], shown as equation (1) below, can be used to calculate heat transfer in biological systems.

$$\rho C_p \frac{\partial T}{\partial t} = \nabla(k\nabla T) + \rho_b C_b \omega_b [T - T_{blood}] + \dot{q} \tag{1}$$

The first term on the right of (1) describes energy transport due to thermal diffusion within the tissue. The second term describes the energy added or removed due to the convective blood flow into and out of the tissue. The third term, $\dot{q}$, represents the metabolic heat generation. In the equation, ρ is the density of the tissue under study, C_p is the specific heat of the tissue, k is the thermal conductivity of the tissue, T is the temperature of the tissue, ρ_b is the density of the blood, C_b is the specific heat of the blood, and ω_b is the blood perfusion rate. T_{blood} is the temperature of the blood.

One goal of this investigation was to successfully incorporate an injected fluid into the COMOSL model. The Bioheat equation can be modified to include the transport of thermal energy by mass flow as shown in equation (2).

$$\rho C_p \frac{\partial T}{\partial t} + \rho C_p \mathbf{u}\nabla T = \nabla(k\nabla T) + \rho_b C_b \omega_b [T - T_{blood}] + \dot{q} \tag{2}$$

The additional term $\rho C_p \mathbf{u}\nabla T$ in equation (2) describes the heat transport in the neural tissue due to fluid flow where **u** represents the fluid velocity.

In addition to using the modified Bioheat equation, conservation of mass and momentum,

equations (3) and (4), are applied to predict the pressure in the neural tissue, as well as the rate of interstitial fluid flow. The conservation of mass equation will also be modified to account for the mass removed by vascular uptake. The fluid velocity, $\mathbf{u}$, is determined using equations (3) and (4) below.

$$\frac{\partial}{\partial t}(\rho\varepsilon) + \nabla(\rho\mathbf{u}) = Q_m \tag{3}$$

$$\frac{\rho}{\varepsilon}\left(\frac{\partial \mathbf{u}}{\partial t} + (\mathbf{u}\cdot\nabla)\frac{\mathbf{u}}{\varepsilon}\right) = -\nabla p + \nabla\cdot\left[\frac{1}{\varepsilon}\left\{\mu\left(\nabla\mathbf{u} + (\nabla\mathbf{u})^{T}\right) - \frac{2}{3}\mu(\nabla\cdot\mathbf{u})\mathbf{I}\right\}\right] - \left(\frac{\mu}{k} + Q_m\right)\mathbf{u} \tag{4}$$

Equation (3) is the continuity equation which is an expression of conservation of mass [10]. In equation (3), ρ is the fluid density, ε is the porosity, and $Q_m$is a mass source term. Equation (4) is a modified version of the Navier-Stokes equations, known as the Brinkman's Interface [10]. Brinkman's law says that the pressure gradient, structure of the medium, and the fluid viscosity are all factors in determining the velocity field. In equation (4), k is the permeability of the porous medium, μ is the dynamic viscosity of the injected fluid, and I is a unit vector. These two equations are used to solve for fluid velocity, and pressure, P; which is used in equation (2) to solve for the temperature and the heat transfer by the injected fluid.

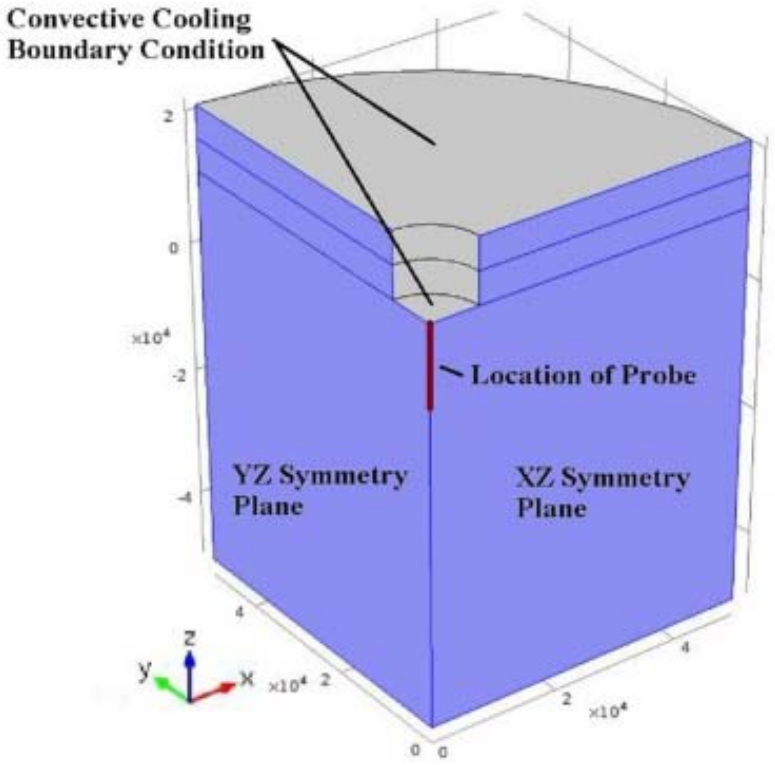

Figure 2: Three-Dimensional Model Space

B. Model Geometry

Figure 2 shows the three dimensional model space used in this investigation. To solve the equations presented in the section above requires the use of a finite element solver. A multiphysics program called COMSOL® was used to perform these calculations using the model space illustrated in Figure 2. COMSOL is able to integrate a number of physics modalities into its calculations to include user inputted differential equations. Additionally, MATLAB (Matrix Labratory) was used to calculate the volumetric heat generation with in the probe using equation 5, further explained below. MATLAB allows the user to write scripts and functions that call upon external and internal variables to accomplish a task. In this case, COMSOL and MATLAB have worked together to couple their programs and allow COMSOL Models to be controlled via MATLAB script, greatly increasing the speed and ease with which model parameters can be adjusted and the subsequent results reported.

Initial modeling took place using a 2-D axisymmetric model, then evolved to the 3-D geometry shown in Figure 2. A 2-D Axisymmetric model is simpler and requires less computational resources. However, it was necessary to determine if a significant change would

occur if the probe was instead modeled as a slab. This difference in geometry is illustrated below in Figure 3.

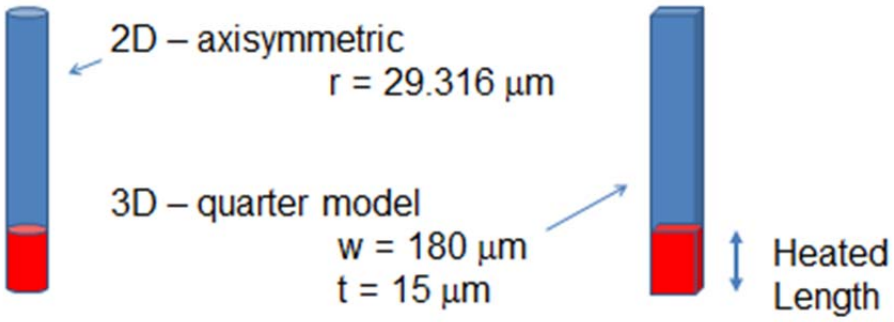

Figure 3: Geometry of probes in 2-D axisymmetric and 3-D quarter models, respectively. The cylinder on the left is how the probe itself was modeled in the 2-D axisymmetric model. The rectangular slab on the right is how the probe was modeled in the 3-D model. The 3-D model modeled the probe more closely to the actual shape of such a probe.

In the 3-D quarter model, the probe was modeled as a rectangular slab, with dimensions based on typical designs from SB Microsystems, knowing that our probe would need to conform to these specifications, and the surrounding tissue is represented as a cylinder. To reduce the model space, a quarter model of the full three-dimensional cylindrical model was created with symmetry boundaries on both the YZ and the XZ planes, as indicated by the axes and highlighted regions in Figure 2. The model also includes both the skull and the scalp in order to represent the proper convective boundary condition above the probe. A "cut" was made through these two overlaying layers in the form of a cylinder in order to simulate the surgical access area required to implant a probe of this design. All of these domains use the Bioheat module of COMSOL® to calculate the heat transfer through the domain while accounting for global blood perfusion and metabolic heat generation based on the properties of each tissue type. Tables 1 and 2 list these properties and their associated sources. The COMSOL® environment includes a number of material properties in its library, some of which were used in this investigation.

To determine if an appreciable difference would be seen between the 2-D axisymmetric model and the 3-D quarter model, both were run under identical conditions. Blood perfusion and tissue metabolism values were ignored and set to 0 in this particular model. The 2-D axisymmetric model appears "upside down" in order to facilitate early MATLAB script functionality. It was

simpler to model the probe's base as the "top" and work down the shank of the probe to the origin. Figure 4, below, illustrates the difference in geometry. The model was run with a boundary temperature of 310.15 (normal body temperature). These models were used to determine if the probe design, as detailed in section III.A, would be effective in physical experiments.

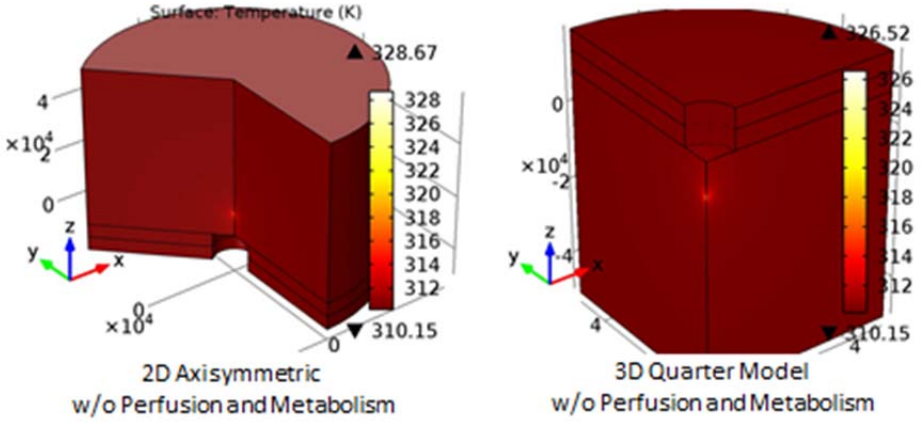

Figure 4: Comparison of 2-D axisymmetric and 3-D quarter model results.

The comparison above shows that the assumption to use a 2-D axisymmetric model for the design of the probe produced similar results, and was reasonable for the designing of a probe capable of inducing ten degrees Celsius increase in tissue temperature (the estimation made by the two models only varied by two degrees. Additionally, Figure 5 below illustrates the temperature distribution as a function of the distance from the center line of the probe. These results indicate that the 2-D axisymmetric model was made under valid assumptions and provides a reasonably accurate characterization of the solution.

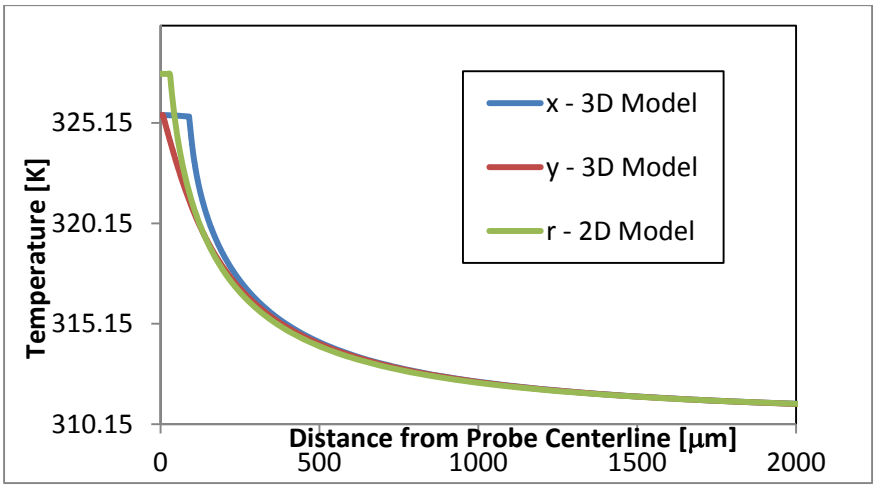

Figure 5: Max temperature vs. distance from the centerline of the probe. This includes both the x and y directions in the 3-D model, and the radius in the 2-D model.

The 3-D quarter model could be solved in a comparable time to the axisymmetric model and more closely represents the physical system, thus the 3-D quarter model was used for further modeling efforts. It is worth noting that at about 500 μm from the probe, the temperature distribution in the tissue is nearly identical for both the 2-D and 3-D models. This is because at that distance, the influence of probe geometry is overcome by the surrounding tissue properties.

Tissues in the body receive the oxygen necessary for cellular function via the blood. At the cellular level, blood is pushed through capillary beds where its bound oxygen can then diffuse across the capillary walls into the surrounding tissues. The rate of flow through these capillary beds is known as blood perfusion. In addition to the effects of blood flow, live tissue will also put out a certain amount of heat due to its own particular metabolism [1]. Table 2 includes the blood perfusion rate and heat generated due to metabolism for each separate tissue. The values for perfusion rate were given in the medical standard units of ml/(min*100g tissue), that is ml of flow per 100 grams of tissue per minute. In order to use this information in COMSOL, these values needed to be converted to the units of g blood/sec*g tissue, that is grams of blood flowing through the area per second per gram of tissue being studied. To accomplish the conversion, the values had to be multiplied by the density of the blood. The metabolism values are representative values, understanding that the metabolism of individual regions of the brain can vary greatly depending on the stimulation of the neurons located in that area. Additionally, although not controlled for in this investigation, adding heat to an area of tissue will cause the tissue metabolism to increase as well [5]. This can make modeling that phenomenon very

difficult, especially on a micro-scale level. For this reason, the assumption of homogeneity and the use of average values helped to eliminate such confounding variables. Table 1 refers specifically to the model space itself and it properties. COMSOL uses the physics module and boundary conditions set by the user to solve the finite element problem. The properties in table 1 are necessary to find a converging solution to the equations presented in the theory section of the paper. Thermal conductivity, heat capacity, and density are basic material properties that must be known in order to understand how a material will conduct heat.

Table 1: Material Properties

Material	Thermal Conductivity k: (W/m*K)	Heat Capacity Cp: J/(Kg*K)	Density : ρ (kg/m^3)
Silicon (Probe)*	130	700	2329
Brain [8]	0.5	3700	1050
Bone (Skull) [8]	1.16	2300	1500
Scalp [8]	0.34	4000	1000

* Properties obtained from COMSOL materials library

Table 2: Perfusion Model Additional Properties

Material	Converted Perfusion Rate (1/sec)	Heat Generation Due to Metabolism (W/m^3)
Brain [8]	0.014	16700
Bone (Skull) [8]	0.00035	368.4
Scalp [8]	0.00032	363.4

C. Probe Model Variables

The dimensions used to generate the probe in COMSOL® are shown below in Figure 6. The variables listed were passed to a MATLAB® script that determined the distribution for the volumetric heat generation along the length of the probe, as described in equations 6 and 7 on page 16 below. This script accounts for both the length of the heated region, Lq_gap, as well as the total input power, qtot (not shown). The position of the origin was chosen to be the tip of the probe in order to better facilitate coupling between the COMSOL® Program and MATLAB® computing environment.

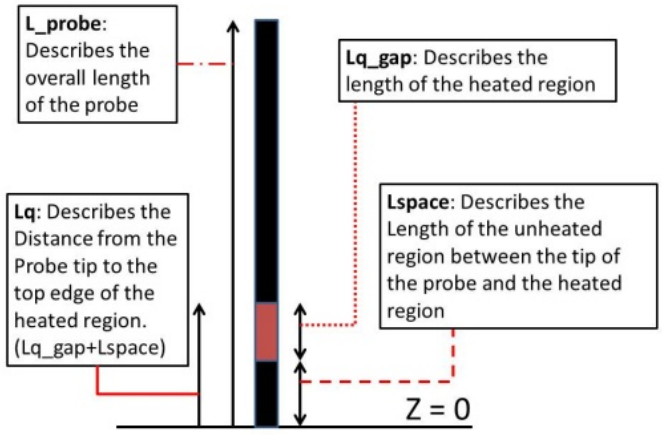

Figure 6: Model probe geometry. This figure locates and defines the main variables that were adjusted for the various parametric studies conducted throughout the course of this investigation.

D. Computed Model Boundary Conditions

Models were run under two different, but related, sets of boundary conditions. The first includes the effects of blood perfusion and tissue metabolism shown in Table 2 above. The boundary conditions for the "live" model, which includes the effects of perfusion and metabolism, are shown in Figure 2. The cylinder walls of this model are insulated, and the heat is removed by blood perfusion in the vicinity of the probe.

The second model does not include blood perfusion and metabolism, and removes the skull and scalp from the model space. This best mimics the conditions of "dead" tissue or a bio-simulant gel. The skull and scalp were removed to facilitate the comparison of the model to the validation experiments conducted with the bio-simulant gel. The cylinder walls were modeled as a fixed temperature of 20 degrees Celsius. The upper surface of the brain tissue was a convection boundary condition.

E. COMSOL 4.3 With Matlab Coupling

COMSOL version 4.3 was used to calculate the temperature excursions for each different scenario throughout this investigation given the user inputted boundary conditions and model geometries. This program offers an additive package to enable coupling functionality with MATLAB, a powerful mathematical processing program with the ability to write specific scripts and call functions. This program's value lies in its ability to simplify COMSOL's task of rendering and running models, as the model space can be defined entirely by code in MATLAB,

preventing the system from having to render wireframe and mesh changes as it would if parametric studies were run within COMSOL itself.

III. PHYSICAL EXPERIMENT

A. Ohmic Probe Design

In order to build confidence in the model, a physical experiment was designed that utilized neural probes which incorporate an ohmic heater at their tip. This particular probe design relied upon simulations run within the COMSOL ® Multiphysics modeling environment. The probe geometry was investigated in a previous study [11] to provide a temperature increase of at least ten degrees centigrade, to reduce measurement error, utilizing an input voltage of five volts.

The probe design, shown below in Figure 7, is a silicon base with roughly 1600 angstroms of deposited material, mostly composed of platinum, on its surface. The probe is roughly 1 cm long, 15 μm thick, and 180 μm wide. The last 620 μm of the probe is the heating portion of the design. By modifying the mask pattern for the platinum layer, heated probes were designed with a serpentine resistive heater on the probe tip, as is illustrated in Figure 7. The serpentine switchbacks on the surface of the probe increase the resistance at the tip, and thereby localize the heated region to allow for the ten-degree temperature elevation. Using resistivity and the geometric properties of the deposited metal layers, the number and length of the resistive elements was determined using a lumped element thermal model for the system to determine the necessary probe resistance assuming a common 5 V source. A lumped element model reduces a problem into discrete components that can subsequently be solved for in more easily computed terms. In this case, the heat transfer through the probe and the necessary amount of resistance was computed by reducing the problem into a representative electrical circuit, with specific components that could thus be quantified and solved. This model assumed that the primary mechanism for heat loss would be conduction into the surrounding tissue and not along the silicon shank of the probe. The platinum thickness was 1500 Å, and the Titanium thickness was 100 Å. The width of the metal lines was limited to a minimum of 5 μm due to the resolution of the metal deposition system available at SB Microsystems, the company that graciously offered to produce and supply the physical probes for this project. SB Microsystems is a biomedical engineering firm that specializes in a number of innovative fields including both macro and micro designs for

medical applications. The resistance of a metal line with resistivity, ρ, length, L, and cross-sectional area, A is given by:

$$R = \rho \frac{L}{A} \tag{5}$$

This probe was fabricated by Scientific and Biomedical Microsystems using existing probe manufacturing processes.

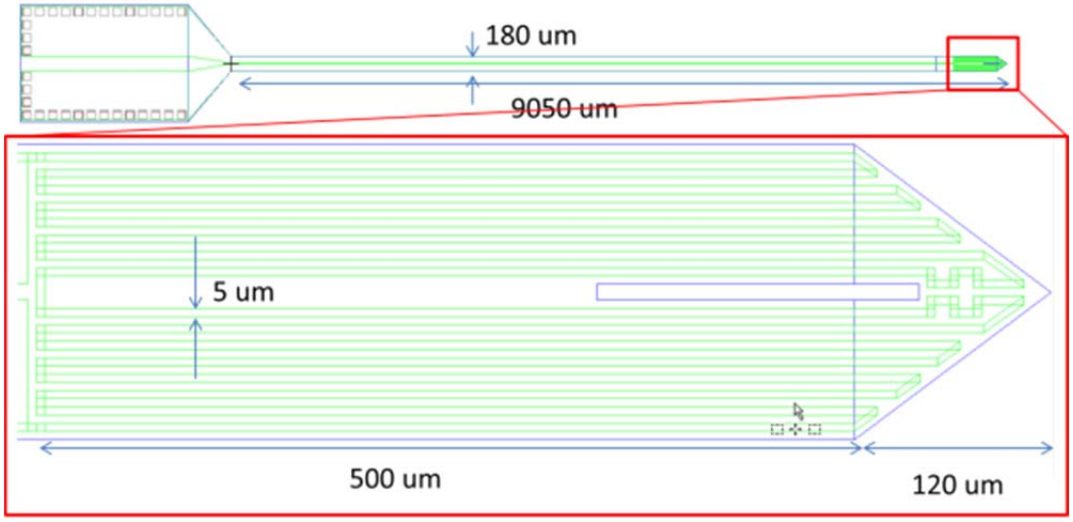

Figure 7: Mask layout for the neural probe containing an ohmic heater to produce a reasonable temperature field for physical experiments.

To establish confidence that this probe design would cause a sufficient increase in temperature, the ohmic heated probe from Figure 7 was modeled in COMSOL using a 2D-axisymmetric model. A number of assumptions were made to allow the use of a 2-D model, rather than a 3-D model in COMSOL. It was assumed that the probe shank was thin enough that there would be little to no resistance to the flow of heat in the transverse direction. It was also assumed that the tissue was homogenous. The 2-D model creates a cylindrical probe, so a radius of 29 μm was entered to maintain the same cross sectional area as the rectangular probe.

For greater accuracy, the COMSOL model was designed to also take into account heating along the shank of the probe due to the leads connecting the heating element at the tip of the probe to the probe base. A MATLAB script was written and coupled to the COMSOL model that took into account the amount of heat output for each lead, as well as the heating elements as a function of the position along the z axis in the model (shown below). The script is essentially a step function that accounts for the geometry at each point and the number and width of the leads or

heating elements. The equation used to create this step function is shown below in equation (7). The volumetric heat generation can be determined using the electrical resistivity, ρ, and the current density, *J*.

$$\dot{q} = \rho J^2 \tag{6}$$

$$\dot{q} = \rho \left(\frac{I}{wt}\right)^2 \frac{N(wt)}{A_x} \tag{7}$$

While the heat is actually generated within the platinum strips, the volumetric heat generation calculated by equation (7) is applied to the entire probe cross-section. This is taken into account in equation (7) by multiplying by the heater cross section and dividing by the probe cross section. *I* is the electrical current, which is calculated form the applied voltage and total resistance using Ohm's law. Equation (7) calculates the heat production per unit volume of the probe along the probe shank as a function of position. *N* refers to the number of elements of identical geometry along a given range of z values. ρ is the bulk resistivity of the platinum, whose thickness is given by the variable *t*. The variable *w* represents the width of the material.

Prior to running the model to determine the effect of the probe, the model space first had to be constructed. In this case, a 2-D axisymmetric system was selected for its more simplified calculation scheme and reduced model space. This cut down on calculation time to allow for initial design work to be more easily modified as the COMSOL environment was explored. The brain is covered by a number of protective layers, the more substantial being the skull and the scalp. These two layers act as insulating boundaries, but in models that include the effects of perfusion and metabolic heat generation, they actually generate a small amount of heat to the model. The model space is shown below in

Figure 9 and includes the boundary conditions used in the COMSOL program for the model excluding blood perfusion.

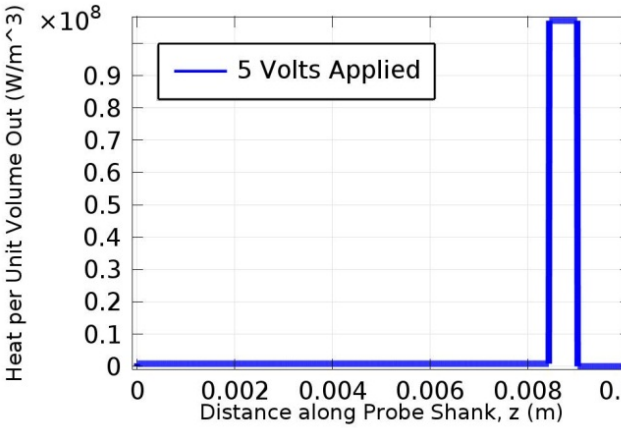

Figure 8: Heat output as a function of z. The long section from z=0 to z=0.0084 is the heat output due to the leads of the probe.

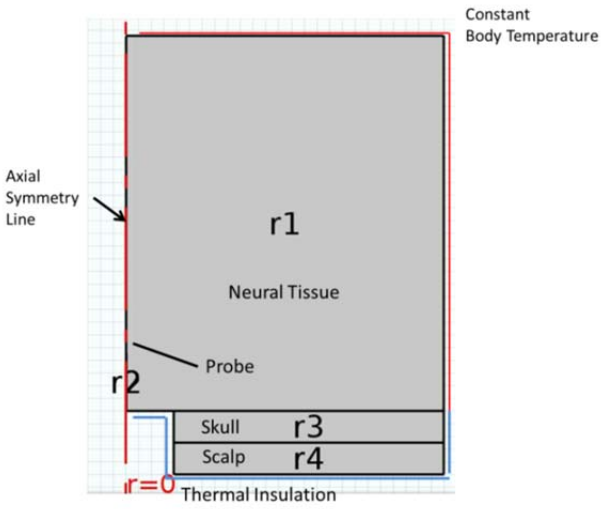

Figure 9: Model Space with boundary conditions not accounting for blood perfusion.

The predicted thermal behavior of these probes is illustrated in Figure 10, with an input voltage of 5V to the probe. The area labeled "Probe" in

Figure 9 was the domain to which the MATLAB script applied the volumetric heat generation of the probe that was calculated given the input parameters and the step function. This model is "upside down" to better accommodate the initial coupled MATLAB script. Utilizing the model space defined in

Figure 9, the system was run to determine the maximum temperature excursion that would be generated by the probe in neural tissue (excluding the effects of blood perfusion and metabolic heat production in the tissue). The results below indicated that the probe design would be successful in future experiments. The effects of blood perfusion and tissue metabolism were purposefully excluded from this model because the physical experiment would not model these effects.

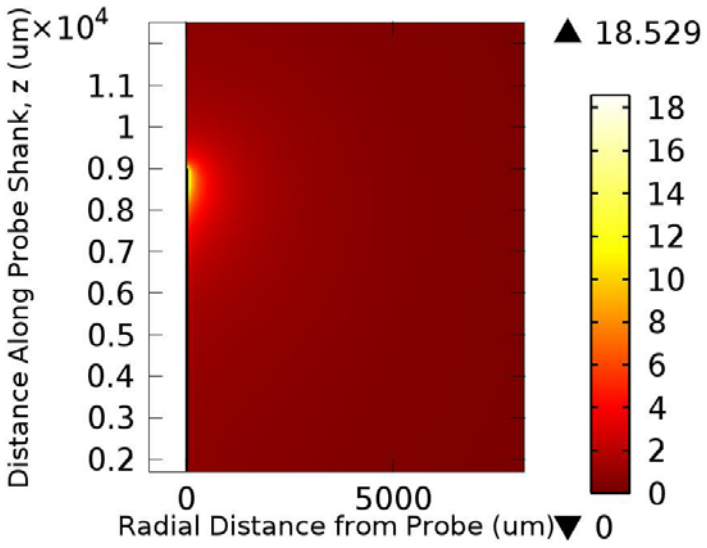

Figure 10: Temperature excursion as calculated for the ohmic heating probe using a 2D axisymmetric model without the effects of blood perfusion and tissue metabolism.

To determine if the models that were generated are accurately portraying the effects of the heating on the tissue, a physical experiment was performed using a neural tissue substitute. An Agar gel matrix was selected as the substitute for this particular investigation. The probes were inserted into this agar gel matrix, explained in further detail below, using the change in resistance of the probe itself to determine the maximum temperature excursion. A composition of 0.65% by weight of Agar which has been used in previous work was used in this investigation [12]. This Agar gel acts as an a simulant of dead tissue, in that it does not provide metabolic heating nor any type of active perfusion. The initial temperature of the gel was set at room temperature and the effects of perfusion and metabolic heat generation were not simulated. Figure 11 below is an image of the actual probes used in this investigation. Probe packaging required the 4X10 SAMTEC connectors be soldered to the probe stalk while protecting the fragile micro-probe from damage. Each probe is unique in its nominal resistance and the pattern in which the electrical pads are connected to the stalk. At first, the probes appeared damaged, as a clear short was present during initial testing. It was determined through experimentation that the issue was in the actual Printed Circuit Board (PCB) Stalk connected to the probe itself. This issue was avoided by removing the pins from the connector prior to soldering the system together. The construction of these probes is such that they are able to be easily inserted into tissue or gel, but

do not do well with bending stresses, and will snap in half with little warning if subjected to such a stress.

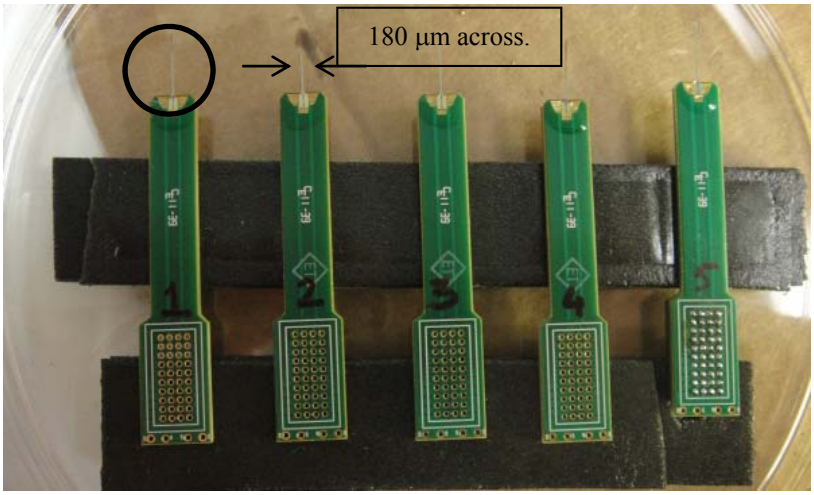

Figure 11: Ohmic heating microprobes provided by SB Microsystems. The area within the circle is the microprobe.

B. Physical Test Platform

The experimental platform shown in Figure 12 was designed and built in-house. A printed circuit board was developed and made to mount the probes using SAMTEC connectors and mounted to a micrometer stage in order to precisely control probe position. The printed circuit board (PCB) was designed and ordered from ExpressPCB. The PCB layout is shown in Figure 13. The resistive probe was used both for heating and for temperature sensing. The temperature is measured by monitoring the resistance of the heater, which is approximately linear with temperature. For this purpose a reference resistor with a nominal resistance of 100.35 ohms was placed in series with the probe resistor and used to transduce the probe current into a voltage. Four wire connectors were placed on the top edge of the PCB in order to facilitate changes in experimental set-up. The SAMTEC connector is a 4X10 pin female socket, SAMTEC number FOLC-110-01-S-Q. The Probe stalk has the male counterpart, MOLC-110-01-S-Q. Four equally spaced holes were placed around the edge in order to attach the PCB to the aluminum sample plate, illustrated below in Figure 13. During set-up, it was discovered that the micrometer stage clearance was not high enough to allow an appreciable amount of adjustment to be made to the PCB, thereby limiting the efficacy of the hardware. This problem was quickly overcome using a fiberglass plate, and 8 standoff screws to directly attach the fiberglass to the mounting plate, and drop the PCB containing the probe down about two inches. All of the screws and nuts

were of plastic construction. An aluminum sample holder was constructed by the USNA Fabrication Lab Technicians with the same dimensions as the COMSOL model cylinder space and filled with 0.65% agar gel. This was subsequently placed in a Precision Microprocessor Controlled 280 Series water bath, manufactured by Thermo Electric Corporation, at room temperature to approximate the constant temperature boundary conditions used in the model. As a data check, the water bath system includes a Traceable® Thermometer with which to calibrate and adjust the water bath microprocessor. Measurements were taken using separate Agilent 34401A $6^{1/2}$ Digit multimeters for the voltage drop across the reference resistor and the input voltage. An Agilent E3620A Dual DC precision voltage source was used to ensure consistent input voltage. The contact resistance for the overall setup was determined to be 0.0004 ohms using a wire short in place of the probe and was subtracted in subsequent calculations to determine the probe resistance.

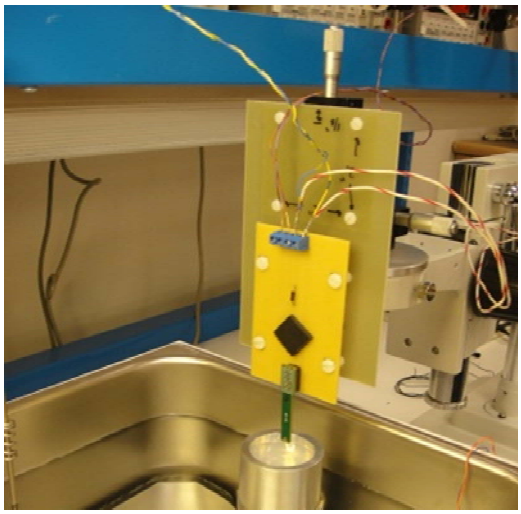

Figure 12: Experimental set-up showing the water bath, aluminum sample holder, and probe connected to the PCB.

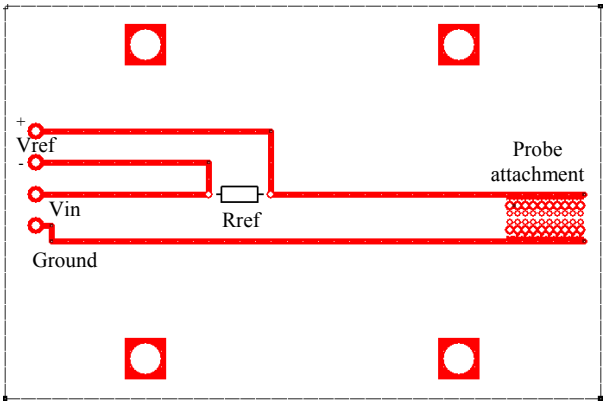

Figure 13: PCB design created in ExpressPCB and used to mount the probe while allowing for specific connections to monitor the voltage drop across the reference resistor.

C. Biosimulant Gel

At first, a hydroxyethyl cellulose gel was considered for use as the biosimulant gel, but the gel did not have the properties expected and needed to mimic neural tissue. The use of agar gel as a brain phantom is not a novel notion. There are numerous studies in which researchers used differing concentrations of Agar gel to mimic either the mechanical or physical properties of neural tissues [12–15]. A concentration of 0.65% was used for this study [12]. Agar gels can be used in a variety of applications depending on the solvent used for the powder. In this case, the gel was measured and added to 100 ml of water prior to placing it in a microwave oven for

roughly 4 minutes. This ensured that the powder dissolved completely prior to allowing the gel to set, which generally took between 10 and 15 minutes. Once set, the gel matrix holds in water, and has a similar heat transfer response to neural tissue as well.

IV. Model Validation

A. Calibration Curve

A calibration curve for the probe resistance as a function of temperature was established by placing the probe in the Precision Microprocessor Controlled water bath, slowly varying the bath temperature, and then recording the temperature and resulting voltage after allowing sufficient time for the system to reach steady-state at each temperature point. For calibration, a low excitation voltage of 0.1 volts was used for measuring probe resistance in order to minimize the effect of the ohmic heater on the readings. This curve was used in all subsequent data collection to translate the resistance of the probe to the temperature of the probe. The water bath was set to room temperature and was checked via the Precision Thermometer at consistent intervals to ensure the system remained at a constant temperature. Two subsequent experiments were performed to compare with model data in the validation process. This curve and its associated equation provide the basis of all subsequent calculations. The error within these measurements carry over into the calculations for the other experiments that depend upon this information. No other temperature detecting system is used for the probe or gel in these experiments. Each probe was calibrated before use. This calibration curve for probe label 1 is shown below as Figure 14

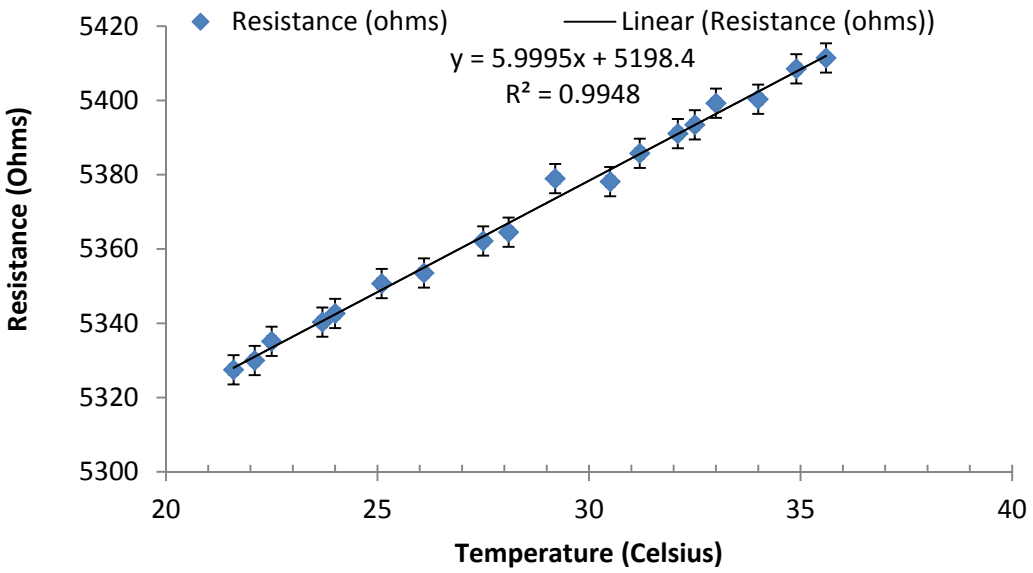

Figure 14: Calibration curve showing Resistance vs. Temperature (C). Error bars are within two standard deviations.

B. Power Dependence Study

Once calibrated, the probe was fully inserted into a 65% by weight Agar gel and allowed to reach steady state. The probe was fully inserted in the center of the gel cylinder. Input voltage was then increased incrementally, each time allowing for steady state to be reached, and recorded. The experimental apparatus was given five minutes to equilibrate fully prior to recording data. The data was then run through a MATLAB script to calculate the resistance of the probe at the set temperature utilizing the voltage measurements taken at the source and across the reference resistor. The mathematical model predicts that temperature will increase linearly with applied power. As shown in Figure 15, the physical experiment corresponded well with the predicted models. The data and the model show similar slopes and linear nature, but they do not match perfectly. It was difficult to maintain a perfectly stable room temperature throughout the test. These fluctuations may have been the major contributing factor for the disparity between the data set and the experimental results. Minor fluctuations aside, the data are in good agreement and therefore provide significant confidence to the solution of the COMSOL model. Input voltage was provided by the Agilent E3620A DC Dual Power Supply system. Voltage readings across the source and the reference resistor were taken by two Agilent 34401A Multimeters.

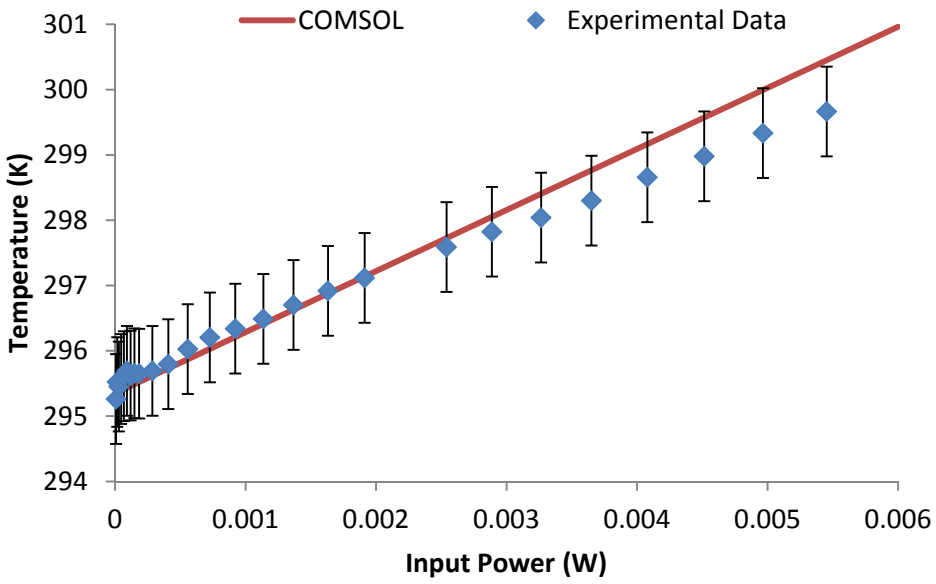

Figure 15: Plot showing experimental data and model results for temperature as a function of input power to the probe. Error bars are within two standard deviations.

C. Insertion Depth Study

For this study, the calibrated probe was incrementally lowered into the gel using a micrometer with a constant input voltage of 5 volts. Voltage was provided by an Aglient E3620A DC Dual Power Supply and both the input voltage and the voltage across the reference resistor were measured via two Agilent 34401A Multimeters. The data was then recorded and entered into a spreadsheet. The input voltage and voltage reading across the reference resistor were then compared against the calibration curve to determine the maximum temperature of the probe at each depth. Data was taken every 3-5 minutes to allow the probe and gel to equilibrate prior to taking the readings. As shown in Figure 16, the predicted model and the physical experimentation agreed reasonably well. The COMSOL model assumes that the heated region at the tip of the probe is fully inserted into the gel, meaning the insertion depth for the COMSOL model will not be below 560 μm. According to both sets of data, the probe reaches a particular depth at which the temperature remains relatively constant regardless of additional insertion, thereby reducing the effect of the cooling at the top surface on the maximum probe temperature.

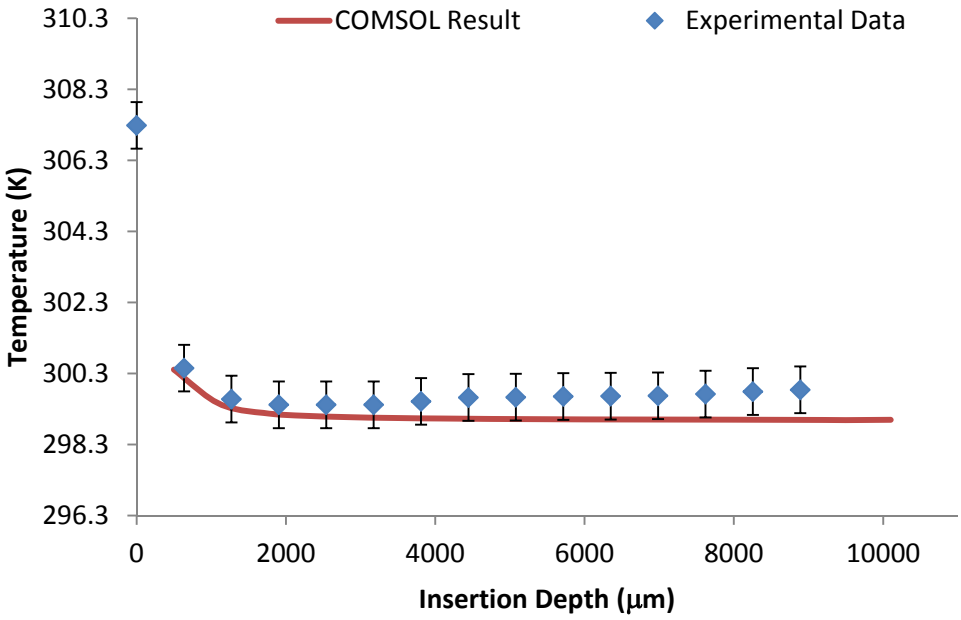

Figure 16: Plot showing experimental data superimposed over COMSOL result for maximum temperature given insertion depth in μm. Error bars are within two standard deviations.

V. Model Predictions and Additional Thermal Modeling

A. Baseline model

The next portion of this study focused on a model that accounted for both blood perfusion and metabolic heating for the purpose of predicting heating in live tissue. In order to do so, a baseline model was first created, then deviations in design were made and the effects observed. The "baseline" model is the primary model from which parameters were adjusted and deviations observed. This served as the control to which each study can be compared. The conditions on which this model was based depended upon a number of factors to include physical and experimental limitations. The initial probe length of 8990 μm was used to mimic the probe that was fabricated based off of the ohmic heating probe design.. It should be noted, however, that neural probe length can vary widely depending on application. The use of a convective cooling boundary for the top planes of the model was set using an average convection coefficient for room temperature and body tissues of 3.6 (W/m^2*K) as reported by de Dear et al. [16]. The value of Lspace, the unheated region between the tip of the probe and the edge of the heater, for this

model was zero so that the heater in the baseline model was completely at the probe tip.. The heated region was 560 μm long.

To determine the input power of the probe, a parametric study was run varying the heat input and recording the maximum temperature. The full results are shown in Figure 17 below. For the baseline model, a heat input value was chosen that would cause a one degree increase in temperature. Ewassif et al. explain that a temperature increase of even one degree Celsius is enough to cause cellular death [5]. This model then served as the baseline for a series of parametric studies described below.

B. *Power dependence*

The effects of adjusting power input are shown in Figure 17. The linear nature of the relationship between applied power and maximum temperature excursion is as expected. The variable in question, qtot, was increased until a temperature excursion of 1 K was reached. The model indicated that the power input needed for a 1 K maximum temperature excursion was 0.75 mW.

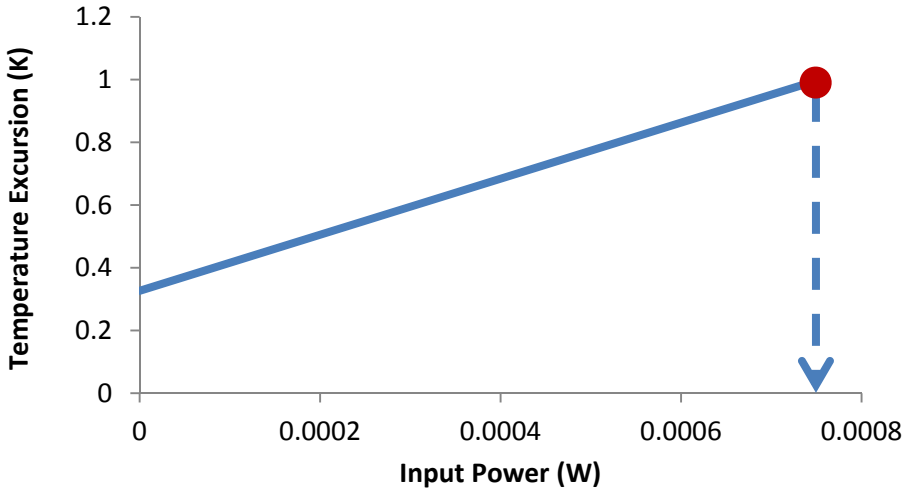

Figure 17: Maximum temperature excursion vs. applied power including effects of blood perfusion and tissue metabolism. This plot illustrates that an input power of roughly 0.75 mW causes a 1 K temperature excursion.

C. *Parametric study of insertion depth*

Due to the wide variability in available probe length, and the effects that convective cooling have on the temperature distribution near the surface of the brain, the insertion depth of the probe

was varied from 1000 μm to 8900 μm in a parametric study in the COMSOL® environment. The results in Figure 18 show that as the insertion depth, and consequently probe length increases, the maximum temperature excursion reaches an asymptotic value. The desired probe depth depends on the nature of the system being studied and stimulated by the probe and should thus be a consideration in thermal management. The length of the heated region, Lq_gap, and the applied power were held constant; and the heated region extended to the end of the probe, Lspace = 0, as previously outlined in Figure 6 The boundary conditions for this particular model were adjusted to account for the convection cooling boundary. When the ambient room temperature is below the temperature of the blood, the surface of the brain is cooled. The ambient room temperature was set to the blood temperature, 310.15 K in Figure 18 to isolate the effect of insertion on the probe temperature.

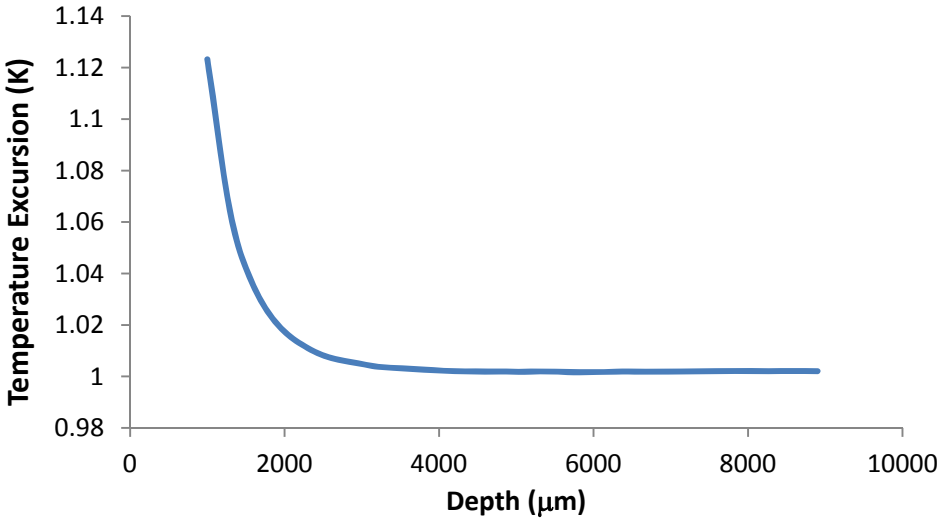

Figure 18: Temperature excursion vs. insertion depth. Model includes blood perfusion and tissue metabolism.

D. Parametric Study of heater length dependence

Another geometric variable to be considered is the length of the heated region in which the power output is located, Lq_gap. A higher value for this variable increases this heated area and results in less localized heat generation, thereby decreasing the observed temperature increase in the surrounding tissue. Figure 19 below displays the maximum temperature increase versus heated region length. This result makes mathematical sense, but has wide implications concerning the design of future probe systems. Point heat sources will create the highest localized heating given a consistent power output. In this case, increasing the area over which

the power is dissipated decreases the maximum temperature excursion because the power per unit area decreases. This principle could be applied to novel probe designs in a number of ways, but one example would be to make the probe thicker to increase the spreading that occurs within then probe. Additionally, making the light source as large as possible for the size of the probe, or using a distributed array of smaller light sources could help prevent more extreme temperatures.

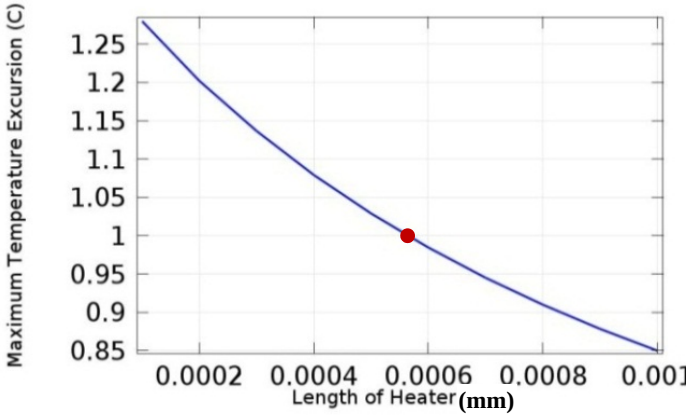

Figure 19: Maximum temperature excursion vs. heater length including effects of blood perfusion and tissue metabolism. The dot marks the baseline model case.

E. Extension of the probe beyond the heat source

The heat source in the previous models has been located on the tip (Lspace = 0). The possibility of the probe acting as a heat dispersing "fin" prompted the investigation of adding probe length to the end of the probe, while keeping the location of the heated region constant. The results of this study indicate that lengthening this tip region (called "Lspace") does create a "fin effect" and reduces the maximum temperature. Figure 20 illustrates the relationship between the unheated tip length and the maximum observed temperature excursion. As expected, there comes a particular length at which the benefit of extending the probe diminishes significantly as the probe begins to act like a fin of infinite length. The optimum extension length in this case, is around 500 to 1000 μm.

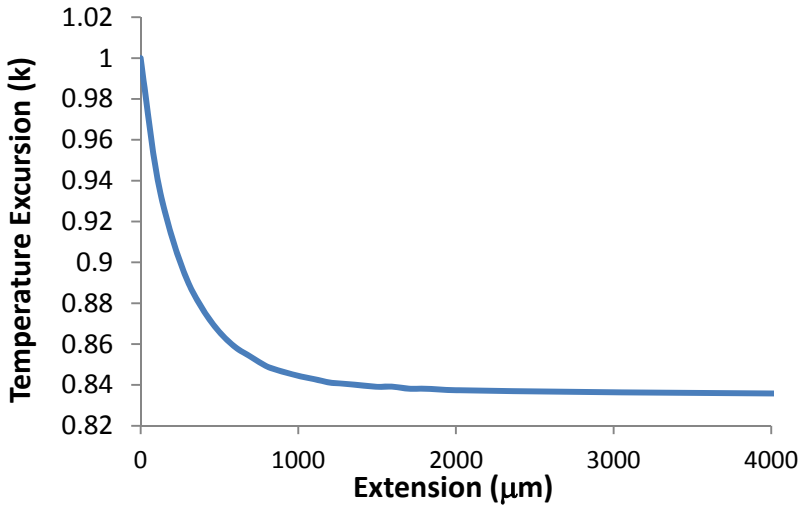

Figure 20: Temperature excursion vs length of probe tip showing that the most effective tip extension is between 500 and 1000 μm.

VI. Injected Fluid Flow

Following the primary probe modeling and physical validation, the model was expanded to include fluid injection via micro-channel within the probe itself. This theoretical channel is modeled in a 2-D axisymmetric geometry with a probe containing an inner radius of 16 μm. The model uses a Brinkman fluid flow computation to first determine the fluid flow through the channel and then into the neural tissue, which has been given a porosity value of 0.2 [13]. Once COMSOL solves for the fluid velocity, it couples the results to the heat transfer module and then solves for the effect of the flow of the saline within the probe and into the tissue. This coupling takes place within a number of MATLAB scripts that first solve for the fluid velocity matrices before using them within Bioheat module. The figures below show the effect of the fluid flow on the temperature of the probe and surrounding tissue.

Probes containing fluid delivery channels already exist and have been used to deliver drugs into live tissues [14], [17]. These designs could be modified to include both injection channels as well as the light emitting source to help mitigate the effects of the heating within the tissue under study.

Below, Figure 21 and Figure 22 display the results of the effect that the flow has on the maximum temperature of the model. The flow model assumes that room temperature fluid is injected at a pressure 10 kPa through a 16 μm radius channel along the 8990 μm length of the probe. The ambient temperature for these models was set to 293.15 K, room temperature, and

the models do not account for metabolism or blood perfusion. With fluid injection, the maximum temperature was reduced by 0.05 K. The temperature reduction could be greater with higher flow rates, the use of chilled fluid, or a distributed outlet flow. While the temperature change for this model was not great, the results demonstrate the potential of the model to further investigate potential mitigation techniques.

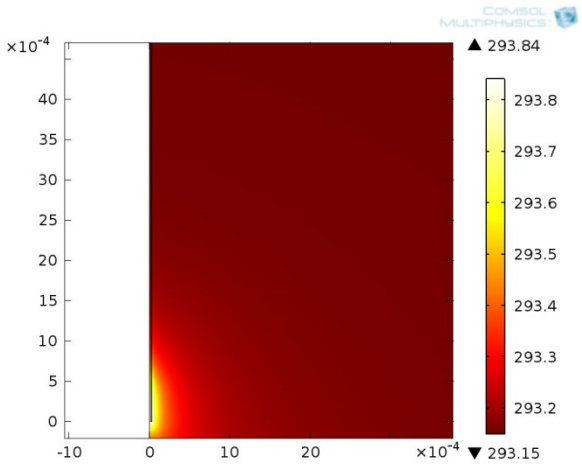

Figure 21: Injected flow model at 10 kPa and input power of 0.00075 W.

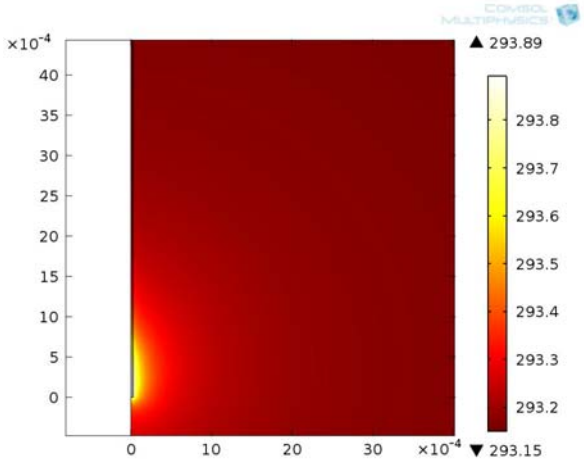

Figure 22: Injected flow model at 0 Pa and 0.00075 W.

VII. SUMMARY

A model for the thermal effects of neural probes that generate heat near the tip of the probe is presented. This model has shown that a number of viable options exist for reducing the temperature changes associated with heat input by an active neural probe. The combination of these effects will allow for a more accurate estimation of the maximum amount of power that can be deposited into neural tissue during use of these systems. This model was validated against an experiment using agar gel as a neural simulant and an ohmic heating probe was designed in house and manufactured by SB Microsystems for the purpose of this investigation.. These probes were calibrated in order to measure temperature. A resistance vs. temperature calibration curve was created and used for each probe. Subsequent models, built on the information gained from this investigation, include blood perfusion and tissue metabolism. Cursory examinations of the possibility of injected fluid flow have been demonstrated and presented. Fluid flow shows some promise, but will require significant work to determine the long term effects of pressuring parts of

the brain. The value of this investigation is a better understanding of the way in which these probes behave. This will allow scientists and engineers to design probe systems that have the least impact on their hosts, thereby allowing for more accurate neural mapping or more effective medical treatments in the future. This work presents the design of these probe systems from a heat transfer perspective, illustrating what could be considered basic guidelines for those researchers looking to create probes with a high intensity of stimulation or in large networks.

REFERENCES

[1] E. P. Widmaier, H. Raff, and K. T. Strang, *Vander's Human Physiology*, 12th ed. New York, NY: McGraw-Hill, 2011, pp. 136–185.

[2] K. D. Wise, D. J. Anderson, J. F. Hetke, and D. R. Kipke, "Wireless Implantable Microsystems : High-Density Electronic Interfaces to the Nervous System," in *Proceedings of the IEEE*, 2004, vol. 92, no. 1, pp. 76–97.

[3] L. Campagnola, H. Wang, and M. J. Zylka, "Fiber-coupled light-emitting diode for localized photostimulation of neurons expressing channelrhodopsin-2.," *Journal of neuroscience methods*, vol. 169, no. 1, pp. 27–33, Mar. 2008.

[4] I.-J. Cho, H. W. Baac, and E. Yoon, "A 16-site neural probe integrated with a waveguide for optical stimulation," in *2010 IEEE 23rd International Conference on Micro Electro Mechanical Systems (MEMS)*, pp. 995–998.

[5] M. M. Elwassif, Q. Kong, M. Vazquez, and M. Bikson, "Bio-heat transfer model of deep brain stimulation-induced temperature changes," *Journal of Neural Engineering*, vol. 3, pp. 306–315, Dec. 2006.

[6] E. S. Boyden, F. Zhang, E. Bamberg, G. Nagel, and K. Deisseroth, "Millisecond-timescale, genetically targeted optical control of neural activity," *Nature Neuroscience*, vol. 8, no. 9, pp. 1263–1268, 2005.

[7] N. Grossman, V. Poher, M. S. Grubb, G. T. Kennedy, K. Nikolic, B. McGovern, R. Berlinguer Palmini, Z. Gong, E. M. Drakakis, M. a a Neil, M. D. Dawson, J. Burrone, and P. Degenaar, "Multi-site optical excitation using ChR2 and micro-LED array.," *Journal of neural engineering*, vol. 7, no. 1, p. 16004, Feb. 2010.

[8] L. Zhu and A. J. Rosengart, "Cooling Penetration into Normal and Injured Brain via Intraparenchymal Brain Cooling Probe: Theoretical Analyses," *Heat Transfer Engineering*, vol. 29, no. 3, pp. 284–294, Mar. 2008.

[9] E. H. Wissler, “Pennes’ 1948 paper revisited,” *Journal of Applied Physiology*, pp. 35–41, 1998.

[10] COMSOL, “COMSOL Help Documentation.” COMSOL Inc, pp. 84–91, 2011.

[11] M. P. Christian, S. L. Firebaugh, and A. N. Smith, “COMSOL Thermal Model for a Heated Neural Micro-Probe,” *Proceedings of the COMSOL Conference, Boston, Massachusetts, Oct. 3-5, 2012*.

[12] R. Deepthi, R. Bhargavi, K. Jagadeesh, M. S. Vijaya, B. Signal, I. Processing, and C. Author, “Rheometric studies on agarose gel - A brain mimic material,” *SAS Tech Journal*, vol. 9, no. 2, pp. 27–30, 2010.

[13] X. Chen, “Convection-Enhanced Delivery of Macromolecule Into Nervous Tissue: Computational Modeling, MR Imagine, and Experiments,” University of Florida, 2008.

[14] C. P. Foley, N. Nishimura, K. B. Neeves, C. B. Schaffer, and W. L. Olbricht, “Flexible microfluidic devices supported by biodegradable insertion scaffolds for convection-enhanced neural drug delivery.,” *Biomedical microdevices*, vol. 11, no. 4, pp. 915–24, Aug. 2009.

[15] E. A. Nunamaker, R. Rathnasingham, and D. R. Kipke, “Viscoelastic Behavior of Rat Cortex in Response to Micro-scale-Volume Fluid Injections,” *Methodology*, vol. di, pp. 1948–1951, 2003.

[16] R. de Dear, E. Arens, H. Zhang, and M. Oguro, “Convective and radiative heat transfer coefficients for individual human body segments,” *Int J Biometeorol*, no. 40, pp. 141–156, 1997.

[17] D. R. Kipke, “Multifunctional Neuroprobes with Integrated Chemical and Electrical Neural Interfaces,” in *Proceedings of the 25th Annual International Conference of the IEEE EMBS*, 2003, pp. 3337–3339.